Optimal Placement and Sizing of IG based DG in Power Distribution System to Reduce Power Losses and Improve Voltage Profile

Idris MUSA[1], Sani M. LAWAL[1], Ganiyu A. BAKARE[2]

[1]*College of Engineering, Department of Electrical/Electronics Engineering, Kaduna Polytechnic, Kaduna-Nigeria*
im4idrismusa@yahoo.co.uk/sanimlawal@gmail.com

[2]*Electrical and Electronics Engineering Programme, Abubakar Tafawa Balewa University Bauchi, Nigeria*
bakare_03@yahoo.com

Corresponding Author: im4idrismusa@yahoo.co.uk

Abstract: In this paper, an extended model of induction machine is developed to provide a simple method for power flow analysis of Induction Generator (IG) for application as Distributed Generation (DG) in distribution network. The power flow analysis allows for ease of computation of the reactive power requirement of the induction generator for subsequent compensation using static compensator devices (shunt capacitors) to relieve the network of unnecessary reactive power demand from IG. The power flow analysis algorithm is combined with AC power flow algorithm (PFA) and particle swarm optimization (PSO) for IG integration in distribution network. The objective is to minimize network power loss. The PFA computes the objective function while the PSO is employed as a global optimizer to find the global optimal solution. The shunt capacitor locally provides the reactive power required by IG. The results of the algorithm, when tested on a standard 33-bus distribution network, show substantial reduction in power loss and overall improvement in network voltage profile.

Keywords: Distributed Generation, Discrete constraint, Particle Swarm Optimization, Power flow algorithm, Induction Generator.

1. INTRODUCTION

Wind driven Induction Generators (IGs) are becoming common sources of Distributed Generation (DG) in distribution systems. This IG-based DG supplies real power and in turn absorbs reactive power from the system. It is therefore necessary to properly model this source for effective integration into the distribution network. An IG is, in principle, an induction motor with torque applied to the shaft, although there may be some modifications made to the machine design to optimize its performance as a generator [1].

IGs are extensively used in many applications due to their simple construction and the ease of their operation. They are more appropriate for some renewable energy applications than synchronous generators because of their lower cost and higher reliability [2]. Several studies have been conducted on the integration of IG-DG in distribution networks. In [3] an analytical technique for optimal placement of wind turbine–based DG in primary distribution systems with the objective of real power loss reduction is presented. The characteristics of wind turbine generation are represented by an analytical expression that is used to solve the DG sizing and placement problem. A PSO-based technique for optimal placement of wind generation in distribution networks is presented [4]. Optimal multiple DG placement using adaptive weight PSO is presented in [5]. Generators of type producing real power at a rate proportional to consuming reactive power from the system are also considered.

The authors in [6] realized the optimal sitting of wind and solar based DG, without considering the sizing. An approach to find the optimum size of DG of three types at optimal power factor is presented in [7], the optimum location for the DG is not solved. A quantum particle swarm algorithm (QPSO) based method for optimal placement and sizing of wind and solar based Distributed Generation (DG) units in distribution system is presented in [8].

However, in [3-8], the reactive power compensation of the IG based DG was not considered. The source of reactive power for IG is the main grid. The result of which is low power loss reduction and voltage profile improvement for the network. It is normally required that the IG is provided with var compensator (e.g. shunt capacitor) at their point of common coupling (PCC) to provide up to 95% of the required compensation.

To address this issue, this paper presents a technique for steady state and power flow analysis of IG. This technique employed the sequence equivalent circuit based on phase frame analysis using matrix equations (6) [9], to compute the reactive power required by IG. The proposed algorithm is combined with AC power flow algorithm (PFA) and PSO for simultaneous integration of IG-DG. The proposed IG algorithm is used to iteratively find the required slip that will force the

real part of the computed complex output power of the generator to be within some small tolerance of the specified output power. The AC PFA software is used to compute the objective function while the PSO is employed as a global optimizer to find the global optimal solution**.** The shunt capacitor is used to provide the reactive power requirement of the IG locally. The imaginary part of the complex power obtained from proposed IG algorithm solution is the required reactive power of IG. The appropriate size of shunt compensation capacitor (SCC) to be located at the IG location is thus, based on this value. The proposed algorithm is found to be effective for simultaneous integration of IG and shunt capacitor when tested on 33-bus benchmarking network. The results showed substantial reduction in power loss and overall improvement in the network voltage profile due to reduction in the reactive power demand from the main grid, as the shunt capacitor is providing above 95% compensation.

The main contributions of this current study are in twofold. First is the implementation of the algorithm for equivalent circuit of the induction machine to compute the reactive power requirement of the generator, instead of the simple empirical formula used in previous studies published in the literature. Second is the inclusion of shunt compensation capacitor(s) as an integral part of the optimisation problem.

2. MODELLING OF IG

In principle, IG can be simply seen as an induction machine with torque applied to the shaft. The extended model of induction machine as generator for power flow analysis and for subsequent network integration is presented in this paper. This involves the steady state and power flow analysis of IG based on phase frame analysis using matrix equations. The developed model based on general mathematical expressions [9] for the phase frame analysis of induction machine and the method used to compute the required slip for the IG based DG are presented in this section.

2.1 Induction Machine Model

The sequence line-to-neutral equivalent circuit of a three-phase induction machine is shown in Fig. 1.
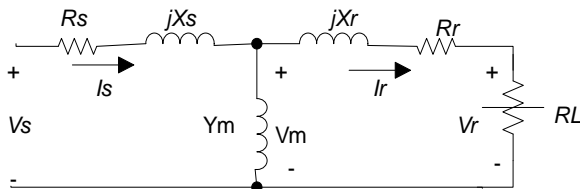
Figure 1: Sequence equivalent circuit

The circuit of Fig. 1 is the result of transformation of the transformer equivalent circuit of an induction machine with the rotor parameters referred to the stator side and is the familiar (Steinmetz) induction machine equivalent circuit. The analysis of the circuit relies on Thevenin's transform to eliminate the shunt branch of the equivalent circuit. This circuit applies to both the positive and negative sequence networks. The value of the load resistance (RL) for each sequence is given by equation (1) [9].

$$RL_i = \frac{1-s_i}{s_i} \times Rr_i \qquad (1)$$

The positive sequence *slip* is given by equation (2):

$$s_1 = \frac{n_s - n_r}{n_s} \qquad (2)$$

where
n_s is the synchronous speed
n_r is the rotor speed

While, the Negative sequence *slip* is given by equation (3):

$$s_2 = 2 - s_1 \qquad (3)$$

The input sequence impedances for the positive and negative sequence networks are determined from Fig. 1 as:

$$ZM_i = Rs_i + jXs_i + \frac{(jXm_i)(Rr_i + RL_i + jXr_i)}{Rr_i + RL_i + j(Xm_i + Xr_i)} \qquad (4)$$

where
i=1 for positive sequence
i=2 for negative sequence

The input admittance for the positive and negative sequence is given by equation (5):

$$YM_i = \frac{1}{ZM_i} \qquad\qquad (5)$$

The input phase complex powers and total three-phase input complex power can be computed from equation (26) - (29) see appendix 'A'.

The above machine model is extended for use in IG with the value of slip been negative. This means that the generator will be driven at speeds higher than the synchronous speed. The generator is modelled with the equivalent admittance matrix [9] and the power flow analysis of IG is implemented in MATLAB and interfaced with MATPOWER AC power flow and PSO algorithms.

2.2   *Computation of Slip*

In DG placement problem, the discrete variable representing the DG sizes are the output power of the IGs. The slip values for the IGs are not known. The goal here is to iteratively find the value of slip that will force the real part of the complex power to be computed for the generator to be within some small tolerance of the specified output power. In this study a tolerance value of 0.001 is used [9].

The procedure is presented in the implementation flow chart of Figure 2 and summarized below;

Step 1: assume initial values of the positive sequence slip and change in slip (initialization of parameters)
Step 2: compute the stator currents, equivalent line-to neutral voltages and the output complex power (3-phase)
Step 3: compute the error as, $Error = P_{speecified} - P_{computed}$
Step 4: check for convergence if satisfied step 7 else Step 5
Step 5: If the error is negative, increase slip else reduce slip
Step 6: repeat steps 2 to 4
Step 7: return the computed complex power

The imaginary part of the computed complex power represents the reactive power required by induction generator.
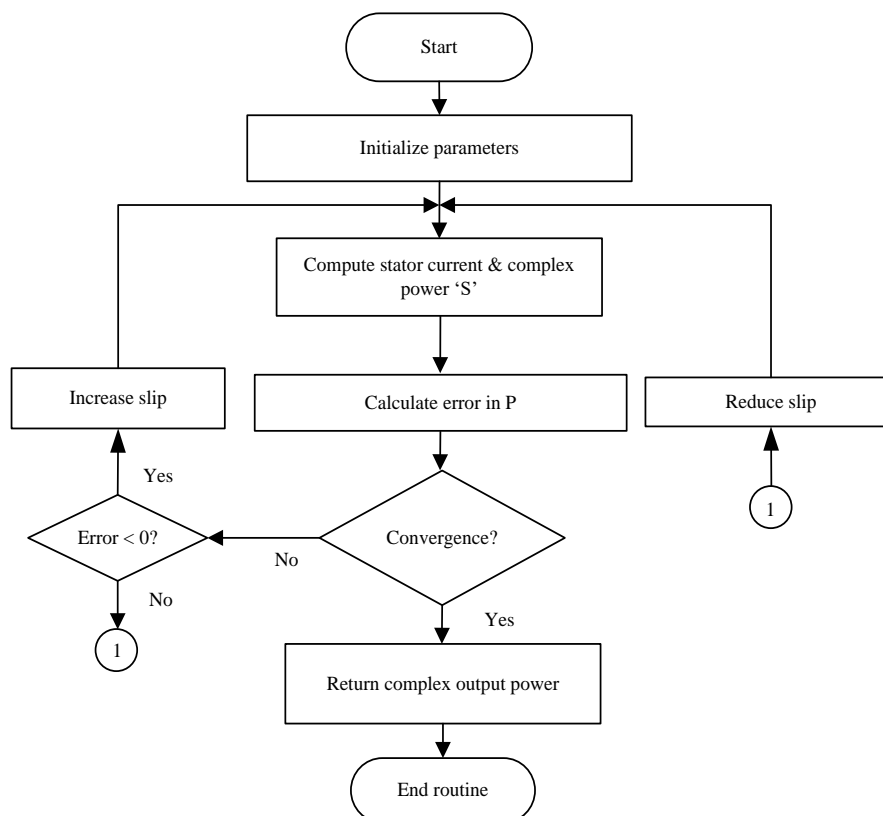
Figure 2: Flowchart for the calculation of induction generator reactive power requirement

3   OBJECTIVE FUNCTION FORMULATION

The objective of this study is to minimize the system power losses by simultaneously integrating an optimal size IG-based DG and shunt capacitor at optimal locations. Connection of an IG- DG unit to a bus is modeled as a negative P and positive Q load. The objective function is computed using MATPOWER AC power flow [10].
The objective function to be optimized can be written as [11]:

$$\text{Minimize } P_L = \sum_{k=1}^{L} Loss_k = \sum_{l \in L} \left(p_{i \to j}^l + p_{j \to i}^l \right) \qquad (6)$$

where L is the total number of branches, P_L is the total real power loss in the network, $Loss_k$ is the power loss at branch k, $P_{i \to j}^l$ is the active power flow injected into line l from bus i and $P_{j \to i}^l$ is the active power flow injected into line l from bus j. Equations (7), (8) and (9) show power, voltage and line current constraints, respectively.

$$\sum_{i=1}^{N} P_{Gi} = \sum_{i=1}^{N} P_{Di} + P_L \qquad (7)$$

$$|\mathbf{V}_i|^{\min} \le |\mathbf{V}_i| \le |\mathbf{V}_i|^{\max} \qquad (8)$$

$$|\mathbf{I}_{ij}| \le |\mathbf{I}_{ij}|^{\max} \qquad (9)$$

where P_{Gi} is the real power generation at bus i and P_{Di} is the real power demand at bus i. $V_i^{\min}$, $V_i^{\max}$ are the lower and upper bounds on the voltage magnitude at bus i. I_{ij} is the current between buses i and j and $I_{ij}^{\max}$ is the maximum allowable line current flow in branch ij.

4.   PARTICLE SWARM OPTIMIZATION

PSO is a population based stochastic optimization technique based on the behaviour of swarms. This algorithm has been successfully applied to solve various nonlinear optimization problems [12]. The swarm is made up of a number of individuals (or particles) with positions in d dimensional space expressed as $X_i = (x_{i1}, x_{i2}, x_{i3}....x_{id})$, where i is the particle number. The particles move within the search space with a velocity $V_i = (v_{i1}, v_{i2}, ...v_{id})$ and with memory of their previous best position, p_{best}, together with the group best position g_{best} until an optimal or near optimal solution is reached. The velocity and position of each particle i at the kth iteration are given by:

$$V_{id}^{k+1} = w^k \cdot v_{id}^k + c_1 \cdot rand_1 \cdot (pbest_{id} - x_{id}^k) + \qquad (10)$$
$$c_2 \cdot rand_2 \cdot (gbest - x_{id}^k)$$

$$x_{id}^{k+1} = x_{id}^k + v_{id}^{k+1} \qquad (11)$$

where rand$_1$, rand$_2$ are uniform random numbers between 0 and 1, v^k is the current velocity of a particle at iteration k and X_{id} is the current position of particle i at iteration k. $pbest_i$ is the previous best position of individual i and $gbest_k$ is the global best of the group at iteration k. c_1 and c_2 are weighting functions that pull each particle towards $pbest$ and $gbest$. w_k is an inertia weight factor that controls the movement in the search space by dynamically adjusting the velocity and can be computed as:

$$w_k = w_{\max} - \frac{w_{\max} - w_{\min}}{k_{\max}} \cdot k \qquad (12)$$

where, w_{min} and w_{max} are the minimum and maximum weights respectively, and k, k_{max} are the current and maximum allowable iteration numbers. The particle velocity and position are confined within the interval $v_{id}^{\min} \le v_{id}^k \le v_{id}^{\max}$ and $x_{id}^k \notin [x_{\min}, x_{\max}]$ respectively.
In this study, the solution vector X in d dimensional space can be expressed as $\mathbf{X}_i = (x_{i1}, x_{i2}, x_{i3}, ... x_{id})$.
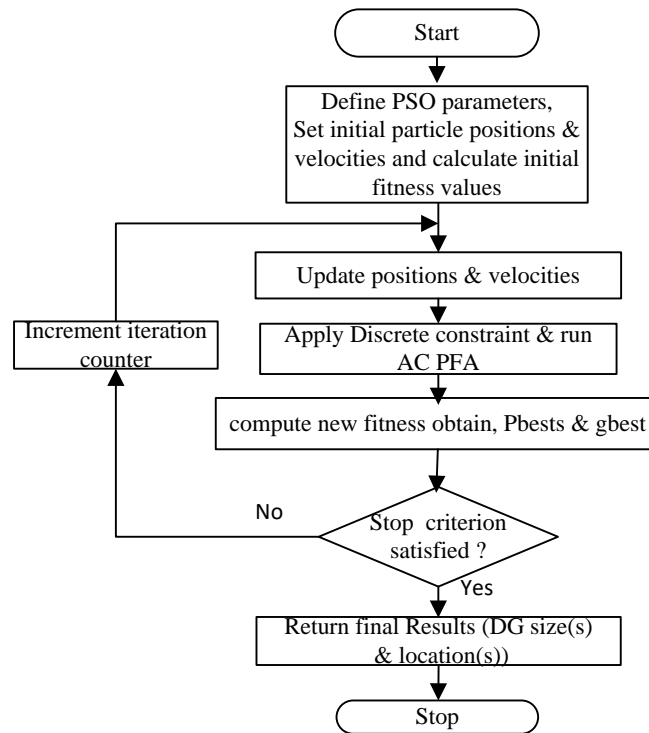
Figure 3: PSO algorithm implementation flow chart

This study is a four-dimensional search space problem and the solution vector is formed as x_1, x_2, x_3 and x_4, where x_1 and x_2 are the DG locations and sizes (output) while x_3, x_4 represent the DG reactive power demand and shunt compensation capacitor. The variables x_2 and x_4 are continuous variables. Due to the discrete nature of the practical IG-based DG and the shunt capacitors used in this study, a discrete variables constraint [13] is applied to the variables x_3 and x_4. These continuous variables are constrained to discrete unevenly spaced variables, using a pre-defined finite search list representing practical IG DG sizes in megawatts. The following PSO parameters are used in this study: $w = 0.7$, $c_1 = c_2 = 1.47$ with a population size of 20. The PSO algorithm implementation flow chart is shown in Figure 3.

5. TEST CASES AND SIMULATION RESULTS

The proposed algorithm was tested on a 12.66kV 33-bus primary radial distribution network (RDN) the feeder is shown in Figure 4. The total substation load is 3.72MW and 2.3MVar, with system data as given in [14]. The base case power loss and reactive power loss in the system are 0.2112MW and 0.1432Mvar respectively.

The test data for the set of IGs used in this study are extracted from [2] and [15] and their summaries are presented in the Tables 5 and 6. They are data (constants parameters) available from the manufacturers of induction machine or those obtained from the results of studies on parameter estimation of IGs as in [2].
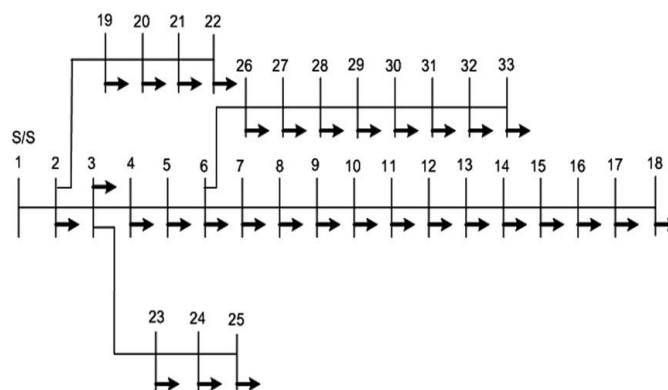
Figure 4: Single line diagram for 33 buses radial distribution test system [14]

Two cases are considered in this study based on 100% load demand on the feeder network i.e. the total real and reactive loads given in Table 1. The first case considered in this study involves the integration of single IG distributed generator without shunt compensation capacitor. The second involves the simultaneous integration of a single generator and a fixed

shunt compensation capacitor. The capacitor size was set to vary between 150kVAr and 4050kVAr with a step size increment of 100kVAr [16]. All the cases are considered with respect to minimizing the total network real power loss.

Table 1: Summary of Results Base Case (no DG connected)

	33- Bus RDN
$\sum$ MW loss	0.2112 MW
$\sum$ MVAr loss	0.1432 MVAr
Min bus voltage	0.9038 pu
Max bus voltage	1.000 pu
$\sum$ load MW	3.72 MW
$\sum$ load MVAr	2.30VAr

5.1   *Test Case I and II*

The first case involves the integration of single IG distributed generator without shunt compensation capacitor. Results of the optimization process using PSO for this case are presented in Table 2. The generator injects 2.0 MW and consumed 0.7607MVAr at bus 6. The second case involves the simultaneous integration of a single generator and a fixed shunt compensation capacitor. Results of the optimization process using PSO for this case are also shown in Table 2. The generator injects 2.3 MW, consumed 2.2396MVAr and compensated with shunt capacitor of 2.15MVAr at bus 6. The voltage profile of the network for both cases is shown in Figure 5. The percentage MW and MVAr loss reductions considering both cases are shown in Figure 6. The voltage profile of the original test network clearly showed that, nodal voltages are an issue under this normal loading condition.

Table 2: PSO Results;33-Bus RDN (Case I and II)

	One DG without shunt capacitor (Case I)	**One DG with shunt capacitor (Case II)**
Optimum bus location	6	6
MWs generated	2. 0 MW	2.3 MW
MVArs consumed	0.7607 MVAr	1.2006 MVAr
Shunt capacitor VAr	-	1.15 MVAr
$\sum$ MW loss	0.1634 MW	0.117 MW
$\sum$ MVAr loss	0.1143 MVAr	0.0852 MVAr
Min bus voltage	0.9264 pu	0.9373 pu
Max bus voltage	1.000 pu	1.000 pu
% power loss reduction	22.62 %	44.57 %
% compensation	0%	95.8%
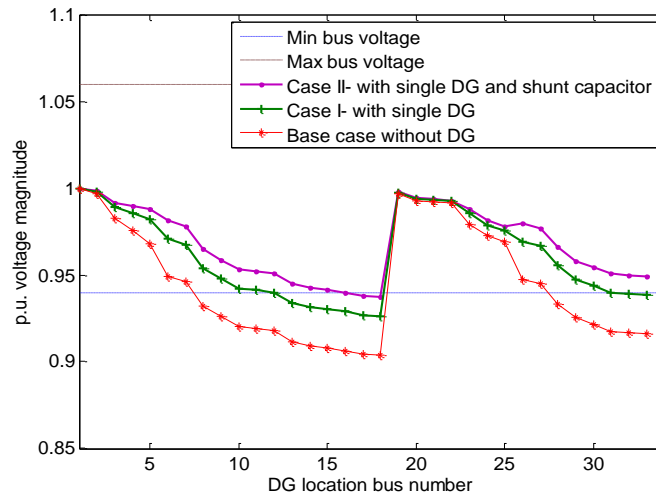
Figure 5: Voltage profile for single optimal IG DG size at optimal location

It is evident from Table 2 that the best loss reduction and voltage profile improvement is obtained with the connection of single DG and shunt capacitor of optimum sizes located at optimum locations (test case II). The shunt capacitor provided 96% compensation for the IG DG locally. This resulted in the relieved of the network and allowing for additional penetration of 0.3MW when compared with case I.
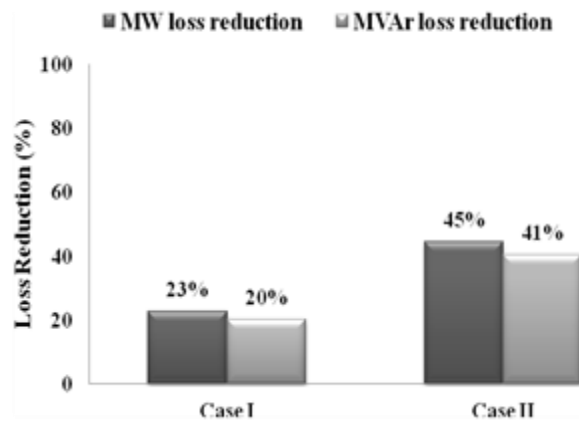
Figure 6: Reduction in power losses: single optimal IG DG without & with shunt capacitor size at optimal location

The result of the power flow analysis of IG for the optimal IG DGs is presented in Table 3. The variation of the slip at different iterations value for the optimal IG DGs is shown in Figures 7 and 8. The positive sequence values correspond to the rated slip values for the optimal DGs.

Table 3: IG Algorithm Results; optimal DG size 33-Bus RDN (Case I and II)

	Complex power & Slips (Case I: without SCC)	Complex power & Slips (Case II: with SCC)
MW Computed	2.0 MW	2.30 MW
MVAr	0.7607 MVAr	1.2006 MVAr
Positive sequence slip	-0.0010	-0.0080
Negative sequence slip	2.0010	2.0080
No of iterations	32	28

The results presented in Table 2 differ slightly from those presented in [4] in which DG size was considered as a continuous variable. In this paper, the PSO algorithm uses a pre-defined list of practical induction generator sizes to define the discrete DG size variable. The discrete step sizes are unevenly spaced. A comparison of the results obtained from the two

algorithms (case 1) is as shown in Table 4. The foregoing discussions of the results have shown that the proposed technique is an effective tool for the integration of IG based DG.
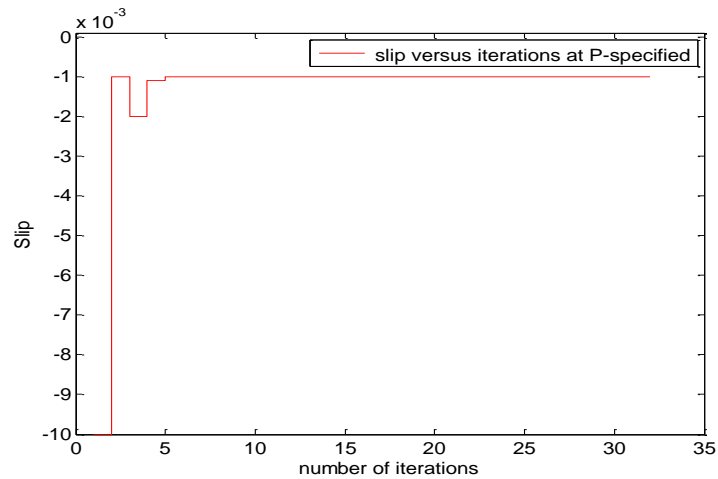
Figure 7: Slip versus Iterations of single optimal IG DG of output 2.0 MW
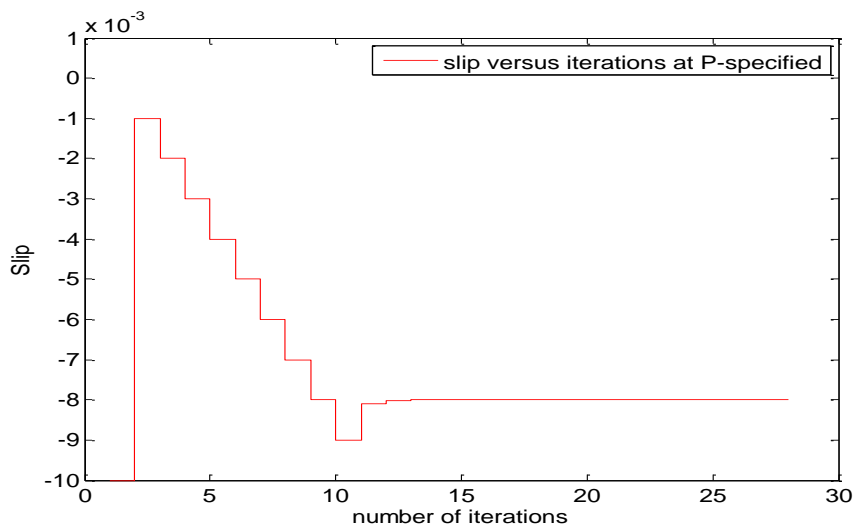
Figure 8: Slip versus Iterations for single optimal IG DG of output 2.3 MW

Table 4: Comparison of PSO Results with those of [4]; optimal DG size 33-Bus RDN (Case I)

	PSO [4]	Analytical [4]	Proposed Technique
Bus location	12	12	6
DG size MW	2.18	1.52	2
MVAr Consumed	0.691	0.592	0.7607
Power loss reduction	26.40%	22.61%	22.62%

6. CONCLUSIONS

An extended model for a three-phase induction machine as generator has been used in this study to demonstrate its application to induction generator integration in radial distribution network. The algorithm developed from MATLAB programming environment was interfaced with MATPOWER AC power flow and PSO algorithm for the integration of induction generator based distributed generation. The study unlike most previous studies has considered the simultaneous integration of IG DG and shunt compensation capacitor. The shunt compensation capacitor locally provided the reactive power requirement of the IG. Thus, resulting in the relieve of the network from unnecessary reactive power demand from the IG, improved network power loss reduction and voltage profile when compared with previous studies. Due to the unevenly spaced discrete nature of the variable representing the IG DG and the evenly step size of the shunt capacitors used

in this study, a discrete constrained was implemented with the PSO algorithm to effectively handle the variables. The proposed algorithm was tested on a standard 33-bus benchmarking medium voltage radial distribution network. The results are obtained under 100% of normal feeder demand with two cases considered. In all cases, the proposed technique was found to be effective in solving the optimization. The best loss reduction and enhanced voltage profile is obtained with single optimally sized and located generators and shunt compensation capacitor. In addition, the use of extended model gives a realistic reactive power requirement of the IG thus, avoiding overestimation or underestimation of the technical benefits of IG integration in distribution network.

ACKNOWLEDGMENT

REFERENCES

[1] Jekins, N., Allan R., Crossley, P., Kirscen, D. and Strbac, G. (2000). *Embedded generation,* London, United Kingdom: The Institution of Engineering and Technology.

[2] Regulski, P., Gonzalez-Longatt F., Wall, P. and Terzija, V. (2011). Induction generator model parameter estimation using improved particle swarm optimization and on-line response to a change in frequency, *Power and Energy Society General Meeting, 2011 IEEE* , pp.1-6, Detroit, USA.

[3] Mahat, P., Ongsakul, W. and Mithulananthan, N. (2006). Optimal placement of wind turbine DG in primary distribution systems for real loss reduction, in Proceedings of Energy for sustainable development: Prospects and Issues for Asia, Thailand.

[4] Satish, K., Sai B. B. R., Barjeev, T. and Vishal, K. (2011). Optimal placement of wind based generation in distribution networks, in *proceeding of IET Conference on Renewable Power Generation,* pp.1-6, Edinburgh, UK.

[5] Prommee, W. and Ongsakul, W. (2008). Optimal multi-distributed generation placement by adaptive weight particle swarm optimization, in *proceeding of International Conference on Control, Automation and Systems,* pp.1663-1668, Seoul, Korea.

[6] Kayal, P., and Chanda, C.K. (2013). Placement of wind and solar based DGs in distribution system for power loss minimization and voltage stability improvement, *Electrical Power and Energy Systems*, 53: 795-809.

[7] Kansal, S., Kumar, V., Tyagi, B. (2013). Optimal placement of different type of DG sources in distribution networks. *International Journal of Electrical Power Energy Systems*, 53: 752-760.

[8] Wanlin, G., Niao, G., Yu, C., Xiaoguang, C., Yu, H., Zhipeng, L., and Jiapeng, C. (2017). Optimal placement and sizing of wind / solar based DG sources in distribution system, *IOP Conference Series: Materials Science and Engineering*, **207** (1) 012096

[9] Kersting, W.H. (2012). *Distribution System Modelling and Analysis,* Taylor & Francis Groups, LLC: Boca Raton London New York, pp.323–339

[10] Zimmerman, R. D., Murillo-Sanchez, C. E. and Thomas, R. J. (2011). MATPOWER Steady-State Operations, planning and Analysis tools for Power Systems Research and Education, *IEEE Transactions on Power Systems*, 26(1), 12-19.

[11] Musa, I., Zahawi, B., Gadoue, S. M. and Giaouris, D. (2012). Integration of Distributed Generation for network loss minimization and voltage support using Particle Swarm Optimization, in *proceeding of 6th IET International Conference on Power Electronics, Machines and Drives*, pp.1-4, Bristol, UK.

[12] del Valle, Y., Venayagamoorthy, G. K., Mohagheghi, S., Jean-Carlos, H. and Harley, R. G. (2008). Particle Swarm Optimization: Basic Concepts, Variants and Applications in Power Systems, *IEEE Transactions on Evolutionary Computation*, 12(2), 171-195.

[13] Clerc, M. (2006). *Particle Swarm Optimization*, London: ISTE Ltd. pp.151–162.

[14] Baran, M. E. and Wu, F. F. (1989). Network reconfiguration in distribution systems for loss reduction and load balancing, *IEEE Trans. Power Delivery*, 4(2), 1401–1407.

[15] Wu, B., Lang, Y., Zargari, N. and Kouro, S. (2011). *Power Conversion and Control of Wind Energy Systems.* John Wiley & Sons, Inc: The Institute of Electrical and Electronics, pp. 319-324.

[16] Abu-Mouti, F.S and El-Hawary, M.E. (2011). Optimal Distributed Generation Allocation and Sizing in Distribution Systems via Artificial Bee Colony Algorithm, *IEEE Transactions on Power Delivery*, 26 (4), 2090-2101.

[17] Musa, I. (2015). Stochastic Optimisation Algorithim with Applications to Distributed Generation Integration," P. hD. Thesis, Newcastle University, Newcastle upon Tyne, United Kingdom

Appendix A
(Derivation of mathematical expressions for extended induction machine model as Generator)

The sequence line-to-neutral equivalent circuit of a three-phase induction machine is shown in Fig. 1.
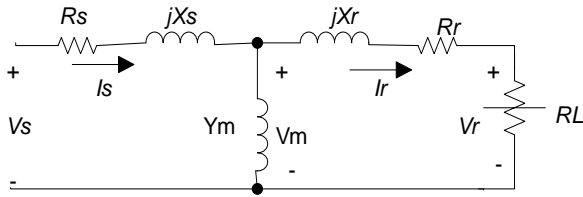
Fig. 1 sequence equivalent circuit

This circuit applies to both the positive and negative sequence networks. The value of the load resistance (RL) for each sequence is given by [6]:

$$RL_i = \frac{1-s_i}{s_i} \times Rr_i \qquad (1)$$

The positive sequence *slip* is given as:

$$s_1 = \frac{n_s - n_r}{n_s} \qquad (2)$$

where
n_s is the synchronous speed
n_r is the rotor speed

While, the Negative sequence *slip* is given as below:

$$s_2 = 2 - s_1 \qquad (3)$$

The input sequence impedances for the positive and negative sequence networks are determined from Fig. 2 as:

$$ZM_i = Rs_i + jXs_i + \frac{(jXm_i)(Rr_i + RL_i + jXr_i)}{Rr_i + RL_i + j(Xm_i + Xr_i)} \qquad (4)$$

where
$i=1$ for positive sequence
$i=2$ for negative sequence

The input sequence admittances for the positive and negative are given by:

$$YM_i = \frac{1}{ZM_i} \qquad (5)$$

The sequence currents are

$$I_0 = 0 \qquad (6)$$
$$I_1 = YM_1 . Van_1 = YM_1 . t^* . Vab_1 \qquad (7)$$
$$I_2 = YM_2 . Van_2 = YM_2 . t . Vab_2 \qquad (8)$$

where

$$t = \frac{1}{\sqrt{3}} . \angle 30 \qquad (9)$$

Since I_o and Vab_0 are both zero, the following relationship is true:

$$I_0 = Vab_0 \qquad (10)$$

Equation (6) through (10) can be put into matrix form as:

$$\begin{bmatrix} I_0 \\ I_1 \\ I_2 \end{bmatrix} = \begin{bmatrix} 1 & 0 & 0 \\ 0 & t^*.YM_1 & 0 \\ 0 & 0 & t.YM_2 \end{bmatrix} . \begin{bmatrix} Vab_0 \\ Vab_1 \\ Vab_2 \end{bmatrix} \tag{11}$$

Equation (11) can be written in shortened form as:

$$[I_{012}] = [YM_{012}].[VLL_{012}] \tag{12}$$

From symmetrical component theory,

$$[VLL_{012}] = [A]^{-1}.[VLL_{abc}] \tag{13}$$
$$[I_{abc}] = [A][I_{012}] \tag{14}$$

Substituting (13) into (12) and the resulting equation into (14) to get

$$[I_{abc}] = [A].[YM_{012}].[A]^{-1}.[VLL_{abc}] \tag{15}$$

The phase frame admittance matrix of induction machine can be defined as:

$$[YM_{abc}] = [A].[YM_{012}].[A]^{-1} \tag{16}$$

Therefore

$$[I_{abc}] = [YM_{abc}].[VLL_{abc}] \tag{17}$$

The input phase currents of the machine from knowledge of the phase line-to-line terminal voltages can be computed using (17). The line-to-line voltages as a function of the line currents are evaluated from (17) as

$$[VLL_{abc}] = [ZM_{abc}].[I_{abc}] \tag{18}$$

where

$$[ZM_{abc}] = [YM_{abc}]^{-1} \tag{19}$$

The equivalent line-to-neutral voltages from line-to-line voltages of equation (18) is obtained as

$$[VLN_{abc}] = [W].[VLL_{abc}] \tag{20}$$

where
$$[W] = [A].[T].[A]^{-1} \tag{21}$$

The matrix W transforms line-to-line voltages to 'equivalent' line-to-neutral voltages. Substituting (18) in (20) to define 'line-to-neutral 'equation:

$$[VLN_{abc}] = [W].[ZM_{abc}].[I_{abc}]$$

$$[VLN_{abc}] = [ZLN_{abc}].[I_{abc}] \tag{22}$$

where

$$[ZLN_{abc}] = [W].[ZM_{abc}] \tag{23}$$

The line currents as a function of line-to-neutral voltages is obtained by taking the inverse of equation (22)

$$[I_{abc}] = [YLN_{abc}].[VLN_{abc}] \qquad (24)$$

where

$$[YLN_{abc}] = [ZLN_{abc}]^{-1} \qquad (25)$$

With equation (22) and (24); machine terminal line-to-neutral voltages and currents known, the input phase complex powers and total three-phase input complex power can be computed:

$$S_a = V_{an}.(I_a)^* \qquad (26)$$
$$S_b = V_{bn}.(I_b)^* \qquad (27)$$
$$S_c = V_{cn}.(I_c)^* \qquad (28)$$
$$S_{Total} = S_a + S_b + S_c \qquad (29)$$

Appendix B
(Induction Generator parameters)

Table 5: Induction Generator's Power & Voltage [2,15]

Machine No.	Pout(hp*746 kw)	Operating voltage (V)		
		Vab	Vbc	Vca
1	330	660	660	660
2	500	690	690	690
3	1000	575	575	575
4	1450	575	575	575
5	1500	690	690	690
6	2000	690	690	690
7	2300	690	690	690
8	3000	3000	3000	3000
9	4000	4000	4000	4000
10	5000	6600	6600	6600
11	6000	4000	4000	4000

Table 6: Induction Generator Impedance Data [2,15]

Seq. No	Rotor impedance (Z_r)ohms		Stator impedance (Z_s)ohms		Magnetizing impedance (Z_m) ohms	
	R_r	X_r	R_s	X_s	R_m	X_m
1	0.010032	0.307428	0.009372	0.100584	0	4.553736
2	0.0093316	0.0589412	0.0033327	0.0451343	0	1.4054472
3	0.003569	0.04516	0.003654	0.04916	0	1.4054472
4	0.00139	0.01565	0.001354	0.03279	0	1.553
5	0.00263	0.04199	0.00265	0.053	0	1.72
6	0.0002381	0.0023805	0.0002381	0.0023805	0	0.71415
7	0.001497	0.0204	0.001102	0.0204	0	0.67052
8	0.018152	0.2949	0.016623	0.2949	0	10.2421
9	0.023152	0.532	0.022104	0.532	0	10.555
10	0.08015	1.13256	0.045302	0.775368	0	41.8176
11	0.02574	0.06854	0.02686	0.07281	0	8.1402